Global NEST Journal, Vol 26, No X, pp 1-11

The modeling of the organic molecules rejection using the bootstrap aggregated neural networks for the evaluation of the forward osmosis process performance

Fouad Kratbi*, Yamina Ammi and Salah Hanini
Laboratory of Biomaterials and Transport Phenomena (LBMPT), University of Medea, Algeria
Received: 24/09/2023, Accepted: 01/05/2024, Available online: 08/05/2024
*to whom all correspondence should be addressed: e-mail: kratbi.fouad@univ-medea.dz
https://doi.org/10.30955/gnj.005404

Graphical abstract

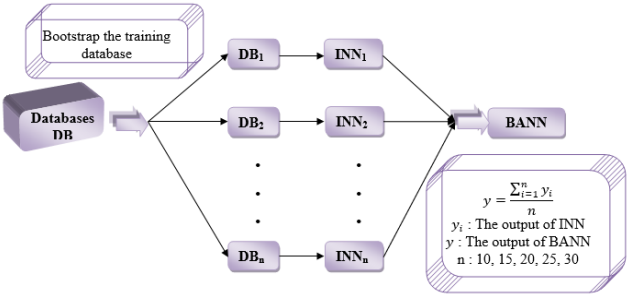

Abstract

The forward osmosis process is currently more studied to be a replacement for another consuming-energy process, for this, many works show up the rejection of different molecules, energy consumption, and modeling of different objectives related to FO process. Our study consists to model the rejection of organic molecules (neutral and ionic) by FO process; however, this paper is the simultaneous applications of the single neural network based on quantitative- structure properties relationship (QSPR-SNN) and the bootstrap aggregated neural network (BANN) to predict the rejection of 53 OM. According to the results obtained, the coefficient correlation "*R*" is used to evaluate the performance of each model for the unseen data, the QSPR-BANN gives *R* value equal to 0.9909 higher than the value of the SNN which is 0.9401, the Root Mean Square Error of the QSPR-BANN is less than that of the QSPR-SNN with values equal to 0.5764% and 1.2826% respectively.

Keywords: Modeling; organic molecules; rejection; bootstrap aggregated neural networks; forward osmosis; membranes

1. Introduction

Membrane separation processes include a large number of techniques for performing separation in different phases (liquid, gas, and mixed-phase) under the action of different driving forces as the potential difference, the electrical, pressure, or chemical potential (Ammi *et al.* 2021; Cordier *et al.* 2020). Microfiltration (MF), Ultrafiltration (UF), Nanofiltration (NF), and Reverse Osmosis (RO) make the main separation membranes process using the gradient of pressure as the driving forces (Zhao *et al.* 2012; Lutchmiah *et al.* 2014). Recently, many works studied the Forward Osmosis (FO) process as the replacement of some techniques (RO and NF) to reduce the energy consumption used to generate the pressure difference (Ammi *et al.* 2021; Cath *et al.*2006; Shaffer *et al.* 2014). The literature highlights several points, in the first place, it is essential to explain correctly the process of forward osmosis with the existence of many models of transfer namely; irreversible thermodynamics, solubilization, diffusion, and pores (Gur-Reznik *et al.* 2008; Lanteri *et al.* 2008). Indeed, forward osmosis presents several interactions between solutes, water, and membranes which complicate the explanation of these phenomena (Chung *et al.* 2012; Martinetti *et al.* 2009; McGinnis *et al.* 2007; Zhao *et al.*2001; Bowen *et al.* 2000; Shetty *et al.* 2003). To solve these problems, new approaches have been proposed to describe nonlinear systems with artificial intelligence which is beneficial by minimization of the number of experiments, reducing financial expenses, saving time, and possibility of modeling systems without profound knowledge (Dornier *et al.* 1995). Artificial Neural Networks (ANN) (Single Neural Networks (SNN) and BANN) have been applied repeatedly to model nonlinear systems by studying the interactions between the molecules, water, and membranes (Ammi *et al.* 2021). However, for the FO process, there are few numbers of studies that use this type of modeling to study the FO system compared with other separation membrane processes such as nanofiltration and reverse osmosis.

The robustness and performance of neural networks have been made the subject of numerous types of research which have used the combination of several neural networks (Bootstrap Aggregated Neural Networks) to develop models in order to ensure the efficacy and

reliability of neural networks generated by the limit of the training phase of the single neural network (Ammi *et al.* 2021; Sharma *et al.* 2009; Zhang *et al.* 2006; Mohammad *et al.* 2020).

Many works used the ANN (Single) to predict the rejection of OM by separation membranes, especially NF and RO membranes (Ammi *et al.* 2015; Yangali-Quintanilla *et al.* 2009), nevertheless, there are few studies that used the ANN to predict the rejection of OM by the FO membranes, (Pardeshi *et al.* 2016) used the ANN to determine the optimum conditions for the FO groundwater desalination, their work gave an honorable result and the ANN used can predict the optimum conditions for the FO system study. Jawad *et al.* 2020 have published a study about the modeling of FO process using an ANN to predict the permeate flux, they studied the effect of nine inputs (membrane (type, and orientation), feed solution (concentration, solution velocity, and solutions temperature) draw solution (concentration, molecule weight, and velocity) on the permeate flux with different parameters of the ANN used (number of neurons, number of the hidden layers), their results obtained were very satisfying and demonstrated its ability to predict the relationships between inputs and outputs in a way better than another simple learning machine such as Multiple Linear Regressions (MLR). Seong-Nam Nam *et al.* 2023 have modeled the permeate flux and the rejection of the Sulfamethoxazole by the FO membranes. In addition, Ibrar *et al*. (2023) have been used a learning machine to predict the permeate flux on the forward osmosis process. On the other hand, no study used the Bootstrap aggregated neural network to predict the FO process compared with the other separation membranes process such as nanofiltration and reverse osmosis processes which are developed with few studies like the studies of Ammi *et al.* (2018, 2021), where they used the QSAR-BANN to predict the membranes performance by treating the removal of pharmaceutical activate compounds, also Khaouane *et al.* (2017), have been studied the rejection of the organic compounds by nanofiltration and reverse osmosis using the BANN.

For the best of our knowledge, our work is the first one using the BANN to predict the rejection of OM by the FO membranes. In summary, many models will be generated with to predict the rejection of OM by FO membranes, SNN will be developed firstly, with the study of the effect of inputs, training algorithms, activation functions, subdivision of the original database, this is the first section of this work, the second section contains the creation of new databases based on the original one with the resampling of its training set to which we will add the testing and validation sets. The QSPR-BANN (stacked of n networks) will be compared between them to get the best performance one, the third section consists to compare the individual neural networks (INN_i) that constituted the best performance BANN model, and the last one is the comparison, in the first hand, between all the models developed in this work, the SNN, the best performance BANN, and the best performance INN, and in the second one, with the other works that used the BANN for the modeling of their works, especially which were about the membrane separation processes. At the end of this work, a conclusion summarizing the results of this work will be investigated.

2. Materials and methods

2.1. Concepts of artificial neural networks (ANN)

The neural network "NN" is a digital technique to bind inputs and outputs data of an external system (process) via a nonlinear regression model established for the best neural network architecture (Mohammad *et al.* 2020). This technique has the aptitude and viability to evaluate the relationships between the inputs and outputs similar to the biological neural networks (Ammi *et al.* 2021). Three stages named input, hidden, and output makes the simple architecture of the NN, the inputs signal received from external sources (bias, *b)* are multiplied by weights (*W*), and if the results of multiplying (*y*) beat the threshold, the signal will be released and sent to the output depending on the NN activation function. In this respect, three steps (training, testing, and validating) are applied to attain the chosen target through NN (Mohammad *et al.* 2020; García-Alba *et al.* 2019). Multi-layer perceptron is a feed-forward backpropagation neural network (FFNN) described by a particular configuration. These neurons are ordered in successive layers and the information runs in one direction, from the input to the output layer, and the neurons of the same layer are not interconnected (Ammi *et al.* 2021; Barello *et al.* 2014; Darwish *et al*. 2007; Madaeni *et al*. 2015; Si-Moussa *et al*. 2008; Maouz *et al*. 2019).

2.2. Bootstrap aggregated neural networks (BANN)

The SNN models are limited by their absence of generalization when applied to unseen data, a good performance has been given by the trained algorithm on the training data and poor performance with data that are not used in this training process. In recent years, many studies have developed new techniques to improve neural network generalization capability such as regularization (Bishop 1991), early stopping (Bishop 1995), Bayesian learning (Mackay 1992), and combining multiple networks (Sridhar *et al.* 1996; Wolpert 1992; Zhang *et al.* 1997; 2008). Among these techniques, the last one (combining multiple networks) is very promising to improve models' prediction on unseen data, this technique consists to develop several neural network models with the aim to model the same relationship and combine them together to progress robustness and performance of the model. The new databases of the bootstrap aggregated neural networks model have been created by sampling the training databases using a function Matlab (bootstrap re-sampling) with replacement to forms 10, 15, 20, 25, and 30 (Ammi *et al.* 2020; Khaouane *et al.* 2017; Zhang *et al.* 2008). Figure 1 shows a BANN, where numerous neural network models are assembled to model the relationship between inputs and outputs, and they are aggregated afterward. The individual networks are learned through using different training data and from different initial

weights. The output of the BANN is a weighted combination of the individual neural outputs (Ammi *et al.* 2021).

2.3. Modeling procedure

This work contains four (04) sections to design and optimize the architecture of the NN as demonstrated in Figure 2. Firstly, the collection, pre-treatment, and analysis of the database. Secondly, the generation a (SNN) model using the original data base with different subdivisions, and different algorithms and functions. The original database is used to create new databases using the re-sampling of its training sets. The new training test assembles with testing and validation sets of the original data to show new data bases. Thirdly, many Individual Neural Networks (INN_i) have been created with the new databases to describe the BANN model. Finally, the comparison and the analysis between the SNN model and BANN model in the first place, and with other works in the second one.

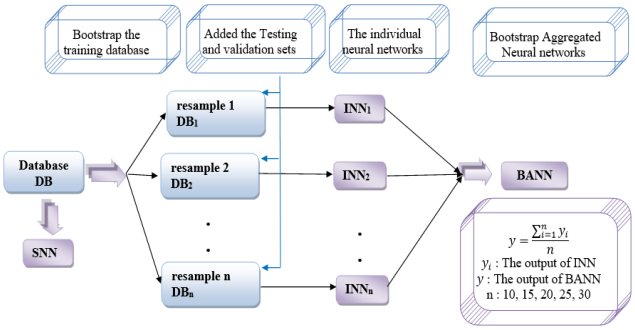

Figure 1. Bootstrap aggregated neural network (Ammi *et al.* 2021)

Table 1. Statistical analysis of the Inputs and Outputs for all databases

	Min	Max	STD	Mean
d_c (g/mol)	0.0914	1.1000	0.1291	0.7917
Log P	0.1612	6.0000	1.2105	2.4347
Dipole moment (Debye)	-2.2200	9.3000	2.9023	2.3499
Length (nm)	0.1468	0.2000	0.0119	0.1579
Width (nm)	0.5000	1.3000	0.1116	0.9969
Depth (nm)	0.3795	1.4000	0.1126	1.0509
Contact angle (°)	42.7	90.3000	6.2294	64.6435
Zeta potential (mv)	-39.91	19.7000	11.9568	-4.3641
pH	3.0000	9.0000	1.5434	6.057
Crossflow Velocity (m/h)	288	1094.4000	388.0198	634.5699
Water flux (l/m2h)	5.2579	17.6000	4.3444	10.0116
Rejection (%)	6.3636	100	14.9789	90.0579

2.3.1. Database; Collection, pre-treatment, and analysis

We have collected a database from the available literature (Alturki *et al.* 2013; Cui *et al.* 2016; Heo *et al.* 2020; Im *et al.* 2021; Jamil *et al.* 2015; Kim *et al.* 2017; Kong *et al.* 2014; Li *et al.* 2020; Lee *et al.* 2019; Linares *et al.* 2011; Madsen *et al*. 2015; Rostgar *et al.* 2020; Xie *et al.* 2014; 2013; Zhang *et al.* 2019), intending to group all the characteristics of the studied system, the size of this database was 193 points of 53 OM. The software "Get data Graph" was used to extract the values of the rejection from the diagram that presented the results. The selection of the input and output variables was based on interactions between the organic molecule's properties, membrane characteristics, and filtration operating conditions for the rejection of the OM by FO membranes. The inputs considered in this work are molecule descriptors (which can be access on the supplementary data, Table S1) (the effective diameter of an organic molecule in water "d_c", molecular length "Length", molecular width "Width", molecular depth "Depth", Dipole moment, The logarithm of the octanol-water partition coefficient "Log P", membrane characteristics (Surface membrane charge as" zeta potential", and the Hydrophobicity "as Contact angle"), and operating conditions (pH, Crossflow Velocity, and the water flux). The values of the effective diameter of an organic molecule in water "d_c", molecular width "Width", and molecular depth "Depth" are calculated with the equations (1), (2), and (3) respectively (Ammi *et al.* 2018; Dolar *et al.* 2012; Santos *et al.* 2006).

$$d_c = 0.065 * M_w^{0.0438} \quad (1)$$

$$Width = \frac{1}{2}\sqrt{S_{min}} \quad (2)$$

$$Depth = \frac{1}{2}\sqrt{S_{max}} \quad (3)$$

Where:

M_w = Molecule Weight.

S_{min}, S_{max} represent the minimum and maximum surfaces area.

The software Hypercham has been used to compute the Log p, Dipole moment, surfaces area and Chembio to calculate the molecular length.

The Statistical analysis is preliminary (standard deviations (STD), minimum, maximum, and mean) is shown in Table 1.

For this database, we used a matrix correlation to edit the interactions between the variables (organic molecule properties, membrane characteristics, and operating conditions) and to reduce its size which can be accessed as Supplementary Data (Table S2).

2.3.2. Development of the QSPR-SNN model

From the original database, serval networks have developed with different subdivisions of the database to find the most performance model of SNN, four (04) subdivisions were used; 80% for the training phase, 10% for the testing phase, and 10% for the validation phase for the first subdivision, the second one was 70% for training, 15% for each other, the third one dived the original data for 60% for the training phase, and 20% for each other, the last one was 90 % for the training phase , 5% for testing, and 5% for validation phase.

For each subdivision, a NN was developed, at first, the training algorithm used was BFGS (Broyden–Fletcher–Goldfarb–Shanno) (Ammi *et al.* 2021; Khaouane *et al.* 2017) quasi-Newton training algorithm and the activations functions in the hidden layer were variants, for this purpose, the Hyperbolic tangent (tangh), the Logarithmic sigmoid (logistic), the sin, and the exponential were used as activation functions for the hidden layer, the Pure linear (purelin) transfer function was fixed and used in the output layer. The number of neurons in the hidden layer was between 3 and 25 neurons for each neural network model.

Software STATISTICA was used for the QSPR-SNN and QSPR-INN$_i$ modeling of the rejection of the OM by the "FO" membranes.

2.3.3. Development of the QSPR-INNi and BANN (Stacked of N networks) models

The development of each QSPR-INN$_i$ was built with a new database, this database was obtained by resampled the training data of the subdivision that gives the most performance of the QSPR-SNN, using the bootstrap re-sampling with replacement to forms 10, 15, 20, 25, and 30. For each one we added the testing and validation sets in aim to obtain a new database.

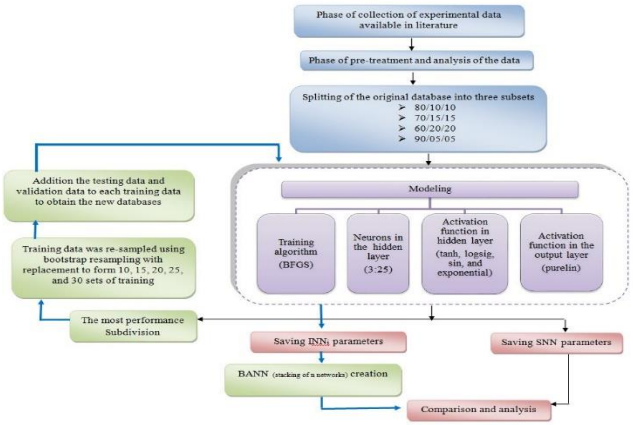

Figure 2. Procedure of design and optimization of the SNN, INN$_i$, and BANN

For each new database, a QSPR-INN$_i$ was modeled Using the same steps that used for the NN model development (same training algorithm, same activation functions, and same various of the neurons number). For each model, several executions were established to extract the final best model, and each execution has been run with a high number of repetitions, sometimes more than 1000 repetitions by execution. The median of the outputs of the QSPR-INN$_i$ gives the stacked neural network QSPR-BANN, the output of the QSPR-BANN was obtained by the following equation (Ammi *et al.* 2021, 2018).

$$y = \frac{\sum_{i=1}^{n} y_i}{n} \quad (4)$$

Where: y represents the output BANN, y_i is the outputs of the individual neural networks, and n is the number of the INN. The software MATLAB is used for resampling and STATISTICA for the creation of the QSPR-INN$_i$.

Table 2. Effect of the subdivision of database

	Phases	Percentage (%)	Errors	
			R	RMSE
Division 1	Training phase	60%	0.7468	10.2087
	Testing phase	20%	0.8459	5.4289
	Validation phase	20%	0.5544	16.4778
Division 2	Training phase	70%	0.9233	5.6799
	Testing phase	15%	0.9397	8.5929
	Validation phase	15%	0.6994	20.0635
Division 3	Training phase	80%	0.8704	6.9761
	Testing phase	10%	0.8818	10.3987
	Validation phase	10%	0.7722	6.5857
Division 4	Training phase	90%	0.9597	4.3432
	Testing phase	05%	0.9400	1.2826
	Validation phase	05%	0.8917	4.3605

3. Results and discussion

3.1. Creation of the QSPR-SNN Model

The original database was divided into three (03) subsets, the main part where the connection weights of the neurons are used to obtain the understanding of the neurons, this is the training data, the generalization ability is proved with the validation data, and the performance of the neural network is established by the testing data.

In order to estimate the influence of the database on the performance of the QSPR-SNN generated, two (02) parameters have been investigated, the correlation

coefficient "R", and the Root Mean Square Error "RMSE", which is given by the next equation (Ammi *et al.* 2021, 2018).

$$RMSE = \sqrt{\frac{\sum_{i=1}^{n}\left(Y_{i,exp} - Y_{i,cal}\right)^2}{n}} \quad (5)$$

$Y_{i,exp}$, $Y_{i,cal}$ represent the experimental and the calculated values respectively; n is the data number.

Table 2 shows the results of the effect of subdivision of the database on the rejection of the organic molecules by forward osmosis "FO" membrane, it is clear that the last subdivision with a percentage of 90% for the training phase, 05 % for testing phase, and 05% for validation phase, gives higher correlation coefficient more than 0.9400 for the testing phase, and with less value of the Root Mean Square Error which equal to 1.2826 for the testing phase. The other subdivisions give acceptable values of the correlation coefficients and RMSE which mean the excellent choice of the inputs of our system studied. For the coming of this work, the subdivision that gives the best performance will be used for the modeling.

The QSPR-SNN model developed is characterized by BFGS quasi-Newton as the training algorithm, the exponential as the activation function in the hidden layer, the Identity (purelin) is the activation function in the output layer, the number of the neurons in the hidden layer is 25, and the number of neurons in the input layers and output layer is 11 and 1 respectively.

3.2. Creation of the QSPR-INNi, QSPR-BANN Models

3.2.1. Performance and comparison between QSPR-BANN

The QSPR-INN_i were developed, as cited previously with the subdivision which has given the best performance of the QSPR-SNN, for this, several new databases have been created using the bootstrap resampling of the training data (90% of the original database), with replacement to form 10, 15, 20, 25, and 30, to which we have been added the testing and the validation data to obtain the new databases. The QSPR-BANN is given by the assembly of the QSPR-INNi models created with the new databases. Table 3 shows the values of the coefficient correlation and the Root Mean Square Error of the testing phase and validation phases for each QSPR-BANN obtained.

For the testing phase (edit the performance of the QSPR-BANN), all the QSPR-BANN have excellent performance with values of "R" more than 0.9500, and small values of the RMSE, the QSPR- $BANN_{(stacking\ 20\ nets)}$ is the model that gives the best performance with correlation coefficient very near to the ideal (R=1) and equal to 0.9909, the Root Mean Square Error equal to 0.5674%. For the validation phase, all the models created have been high values of the correlation coefficient, and small values of the RMSE which demonstrate the generalization ability for predicting the organic molecules rejection by the forward osmosis "FO" membranes of all the QSPR-$BANN_{(stacking\ of\ n\ nets)}$ generated.

Table 3. Values of "R" and "RMSE" of testing phase and validation phase for each QSPR-BANN

QSPR-BANN	Errors			
	Testing Phase		Validation phase	
	R	RMSE	R	RMSE
$BANN_{(stacking\ 10\ nets)}$	0.9618	0.9465	0.9741	6.6946
$BANN_{(stacking\ 15\ nets)}$	0.9850	0.9727	0.9778	4.5866
$BANN_{(stacking\ 20\ nets)}$	0.9909	0.5764	0.9646	4.8274
$BANN_{(stacking\ 25\ nets)}$	0.9823	0.8201	0.9782	6.1380
$BANN_{(stacking\ 30\ nets)}$	0.9839	0.7998	0.9774	6.3269

In addition to the previous discussion, other values of errors are used to evaluate the performance of the QSPR-$BANN_{(stacking\ 20\ nets)}$. For that, a comparison with the other QSPR-BANN developed using the mean absolute error (MAE), the root mean squared error (RMSE), the model predictive error (MPE), and the standard error of prediction (SEP) of the QSPR-BANN obtained on the testing phase, and validation phase. The performance of the model is based on the values of these errors, where for the values less than 10% the performance is excellent, between 10% and 20% the performance is good, fair performance for values between 20% and 30%, and low performance if the values are more than 30% (Amiri *et al.* 2020; Despotovic *et al.* 2015; Fissa *et al.* 2019). These errors are obtained with the following equations (Ammi *et al.* 2021; 2020; Zhang *et al.* 2019).

$$MAE = \frac{1}{N}\sum_{i=1}^{N}\left|\left(y_{i,exp} - y_{i,cal}\right)\right| \quad (6)$$

$$RMSE = \sqrt{\frac{\sum_{i=1}^{N}\left(Y_{i,cal} - Y_{i,exp}\right)^2}{N}} \quad (7)$$

$$MPE(\%) = \frac{100}{N}\sum_{i=1}^{n}\left|\frac{\left(y_{i,exp} - y_{i,cal}\right)}{y_{i,exp}}\right| \quad (8)$$

$$SEP(\%) = \frac{RMSE}{Y_e} \times 100 \quad (9)$$

$Y_{i,exp}$, $Y_{i,cal}$ represent the experimental and the calculated (predicted) values respectively, n is the number of data, and Y_e is the mean value of the experimental data.

As shown in Figure 3. For the testing phase, it is clear that the QSPR-$BANN_{(stacking\ 20\ nets)}$ has a small value of error than the error QSPR-BANN with MAE equal to 0.5001%, RMSE equivalent to 0.5764%, MPE equal to 0.5179%, and

SEP value is 0.5986%. These results give a higher performance of the QSPR-BANN $_{(stacking\ 20\ nets)}$ generated.

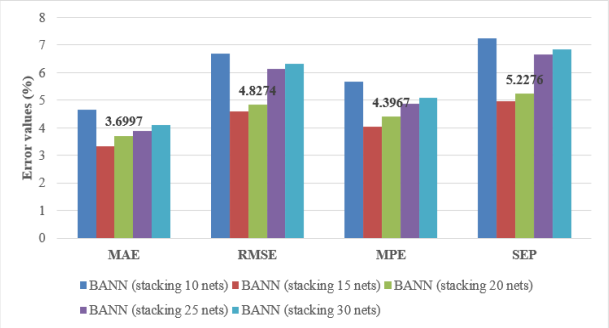

Figure 3. Parameters of performance of the QSPR-BANN for the testing phase

For the validation phase, as mentioned in Figure 4, the QSPR-BANN $_{(stacking\ 20\ nets)}$ has a value of the errors near the smaller value (QSPR-BANN $_{(stacking\ 15\ nets)}$) and less than the other QSPR-BANN with values equal to 3.6997%, 4.8274%, 4.3967%, and 5.2276% for the MAE, RMSE, MPE, and SEP respectively, which means that the generalization ability of the QSPR-BANN $_{(stacking\ 20\ nets)}$ and (QSPR-BANN $_{(stacking\ 15\ nets)}$) is the best in comparison with other QSPR-BANN developed.

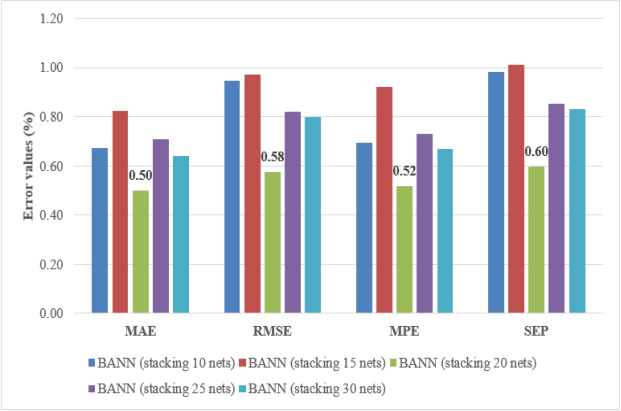

Figure 4. Parameters of performance of the QSPR-BANN for the validation phase

3.2.2. Performance and comparison between QSPR-INN$_i$

The previous section 3.2.1 has demonstrated that the QSPR-BANN $_{(stacking\ of\ 20\ nets)}$ gives the most performance model among the other QSPR-BANN.

The structures of the INN developed change from one model to another. It is clear that the log sigmoid present the activation function the most using as the transfer function with eight (08) individual neural networks, seven (07) individuals were used the tangent hyperbolic (tangh) as the activation function in the hidden layer, and the exponential function which gives the performance of the SNN model as cited previously has been used by five (05) individual neural networks, and while neural networks used the sin as the activation function in the hidden layer. It can be summarized that the two activation functions (tangh and logistic) are in the majority in comparison with the two other functions (Exponential and sin), these results are in accordance with the other works on the same targets.

The INN (5, 6, 8, 10, 14, 15, 17, and 19) have a number of the neurons in the hidden layer (determined by empirical rules) identical to or less than the number of the neurons in the input layer, the other individual neural networks have a number of neurons more than the number of the input (11) similar as the QSPR-SNN model. In addition to the previous discussion, a rule of Dames 2005 gives a relationship between the number of the inputs and the number of neurons in the hidden layer, it can be equal to the number of inputs (11 neurons in our case); equal to 75% of the number of the inputs (8 neurons in our work); and equal to the square root of the input and output (11 neurons in our study), the INN with a number of neurons less than 11 are harmony with this rule. Also, to guarantee that the variables of the neural models do not surpass the size of the database we test the next rule cited by ((the inputs * the number of the hidden layer) + (the number of the hidden layer* the outputs)) ≤ the dimension of the database, for this, the twenty individuals neural network give respectively (192, 218, 156, 251, 36, 66, 192, 132, 165, 132, 253, 218, 240, 108, 36, 180, 36, 144, 84, 192) where the size of the database is more than 2123 (Fissa *et al.* 2019). Table S3 represents the values of the previous parameters of evaluation of the performance (MAE, RMSE, MPE, and SEP) in addition to the correlation coefficient of the all QSPR-INN$_i$ for the training phase, testing phase, validation phase, and total phase.

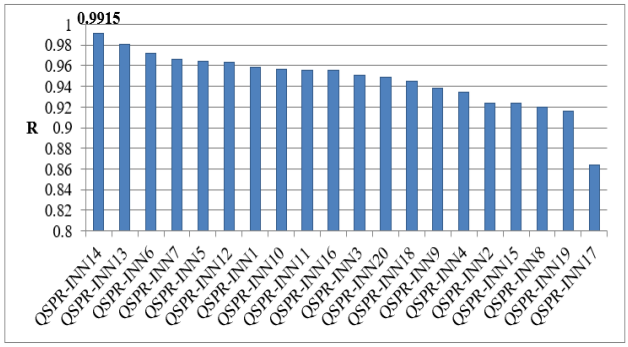

Figure 5. Coefficient correlation of twenty (20) INN$_i$ for the testing phase

According to this Table, it is obvious that each INN has different values of previous parameters (R, MAE, RMSE, MPE, and SEP), which means the not dependable of the individual neural networks developed. Figure 5 shows the descending order of the coefficient correlation values, the INN_{14} has the highest value of "R" more than 0.9900 and equal to 0.9915, and five (05) INN give excellent performance with values of "R" more than 0.9600, eleven (11) INN have a good performance with values of R between 0.92 and 0.96, two (02) have acceptable performance with values of R from 0.91 to 0.92, and one (01) individual neural has poor performance with a value of "R" equal to 0.8642.

The precision of the INN can be extracted from the following figures, where, for the MAE as cited in Figure 6, it can be shown that only one individual neural network has a value of MAE more than 2%, eleven (11) between 2% and 1%, and the others have a good precision with values less than 1%. The best performance individual

neural network INN_{14} has the best precision with a value of MAE equal to 0.9749%.

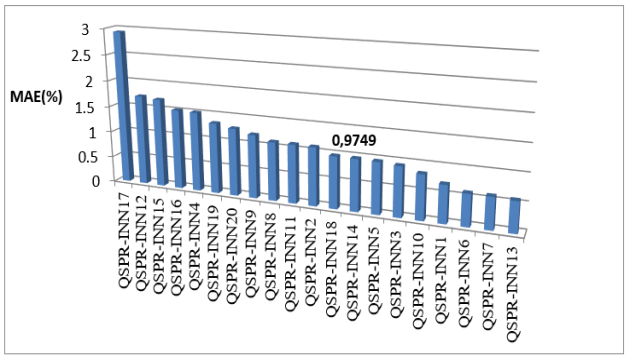

Figure 6. MAE of twenty (20) INN_i for the testing phase

The ascending order present in Figure. 7 explains that the majority of the INN have good precision, except for two individuals which have values of the RMSE greater than 2%. The best performance individual INN_{14} gives good precision with a value of RMSE equal to 1.1552%.

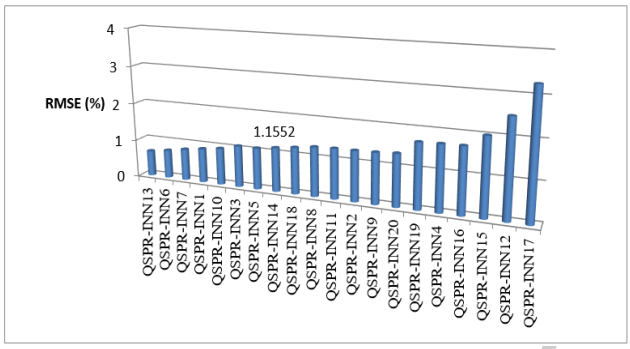

Figure 7. RMSE of twenty (20) INN_i for the testing phase

The values of MPE as mentioned in following Figure 8 explain that the minority of the individuals have higher values of MPE (more1.5%) which demonstrates the good precision of the INN generated, the most performance INN_{14} has been represented with a small value of MPE equal to 1.007%.

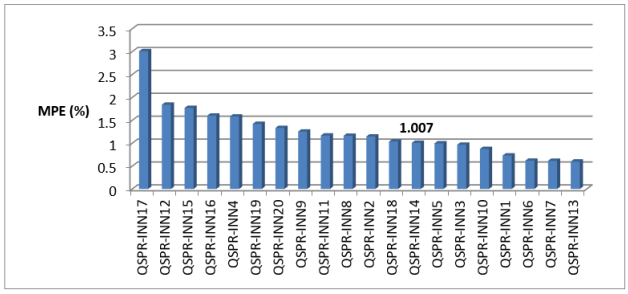

Figure 8. MPE of twenty (20) INNi for the testing phase

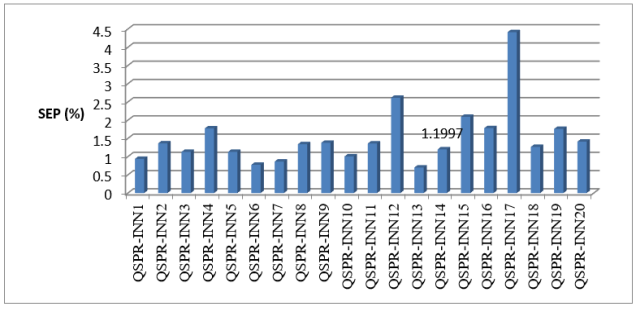

Figure 9. SPE of twenty (20) INN_i for the testing phase

The twenty (20) neurals developed have different values of SPE as mentioned in Figure 9, where, three (03) INN_i have values more than 2%, eleven (11) between 1% and 2%, and six (06) INN_i with SPE values less than 01%. The best performance individual neural network has a value of SPE equal to 1.1997%.

3.3. Performance, comparison, and analysis of the NN models

3.3.1. Comparison between BANN, INN_i, and SNN

According to the previous discussion, many NN models were developed (QSPR-SNN, QSPR-BANN $_{(Stacking\ of\ n\ networks)}$, and QSPR-$INN_i$) with the aim of modeling the rejection of OM by FO membranes.

The previous sections, 3.2.1 and 3.2.2 demonstrated that the QSPR-BANN $_{(Stacking\ of\ 20\ networks)}$ and QSPR-INN_{14} are the most performance models between the QSPR-BANN $_{(Stacking\ of\ n\ networks)}$ and the QSPR-INN_i respectively. In this next section, a comparison between these two models (QSPR-BANN $_{(Stacking\ of\ 20\ networks)}$ and QSPR-INN_{14}) and QSAR-SNN is carried out.

The scheme and the factors of the linear regression have been, directly, given by the Matlab function "Postreg". Figure 10 depicts a comparison between experimental and calculated rejections for each model with agreement vectors approaching the ideal [i.e. α= 1 (slope), β= 0 (intercept), R= 1 (correlation coefficient)] in the adjustment of the profiles of the neural networks, for SNN ([α, β, R] = [0.6200, 34, 0.89173] for validation phase and [α, β, R] = [0.7700, 22.00, 0.94008] for test phase, for QSPR-BANN $_{(Stacking\ of\ 20\ networks)}$ ([α, β, R] = [1.3, -31, 0.96462] for validation phase and [α, β, R] = [0.89, 10, 0.99095] for test phase), and for QSPR-INN_{14} ([α, β, R] = [1, -3.5., 0.91837] for validation phase and [α, β, R] = [1.2, -21., 0.99154] for test phase). The slop α is equal to 1 for the validation phase in QSPR-INN_{14} and it is close to 1 for the validation phase in the QSPR -SNN and QSPR-BANN $_{(Stacking\ of\ 20\ networks)}$ models, it is very close to 1 for the testing phase in both neural networks models. The intercept β is very far from 0 for the validation phase and testing phase in the QSPR -SNN, QSPR-BANN $_{(Stacking\ of\ 20\ networks)}$, and QSPR-$INN_{14}$ models except that the value of The intercept β for the validation phase in the QSPR-INN_{14} which is close to 0. Correlation coefficients have generally reflected the excellence of models where their values between ($0.90 \leq R \leq 1.00$), for these neural networks generated (QSAR-SNN, QSAR-BANN $_{(Stacking\ of\ 20\ networks)}$, and QSAR-$INN_{14}$), the values of the correlation coefficients are very close to the ideal value (R=1) and lead us to show the good robustness of the established neural models and the possibility of predicting the different parameters that characterize the rejection of organic molecules during forward osmosis process.

Figure. 11 shows the comparison between the three models, it can be seen that for all the errors used in the comparison, the BANN $_{(stacking\ of\ 20\ networks)}$ is the model which has the best precision than the others (SNN, and INN_{14}) for testing phase with values of MAE less than 1% for all models, RMSE equal to 0.5764% for BANN and

more than 1% for SNN and INN_{14}, the MPE has near values for SNN and INN_{14}, the BANN (stacking of 20 networks) has fewer values than them with values equal to 0.5179%. The SEP as shown in the same Figure 11 takes the same rule with values equal to 0.5986% for the BANN (stacking of 20 networks), between 1% and 1.2% for INN_{14}, and more than 1.2% for SNN.

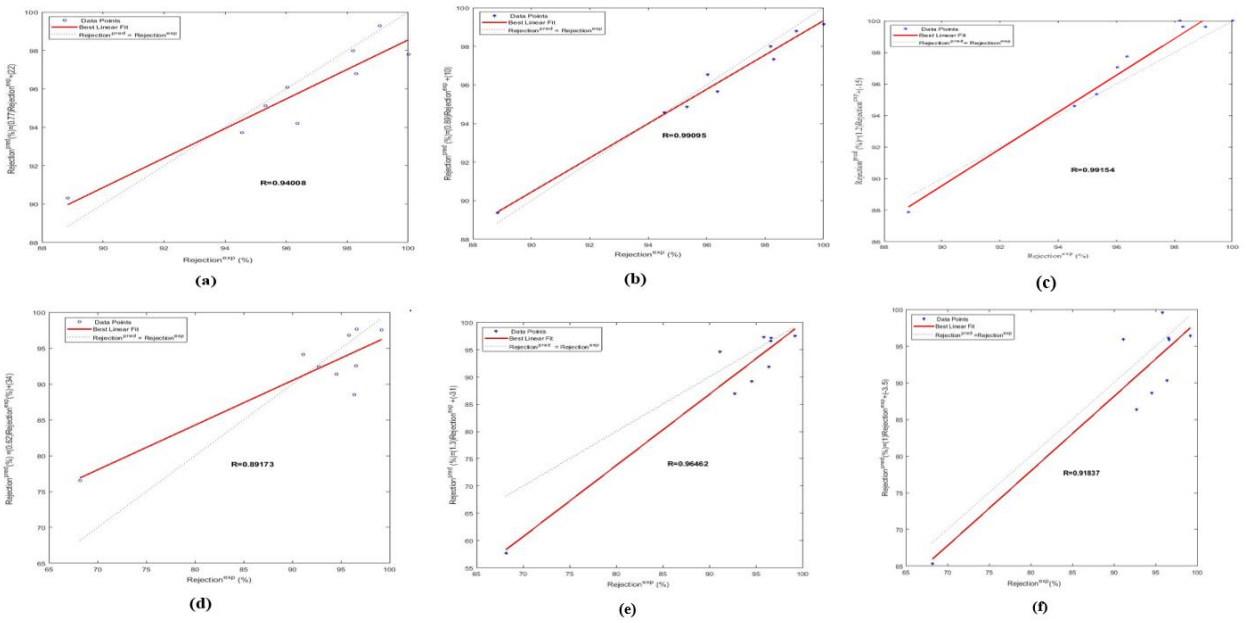

Figure 10. Plot of linear regression: (a) testing phase for SNN, (b) testing phase for BANN (stacking of 20 networks), (c) testing phase for INN14, (d) validation phase for SNN, (e) validation phase for BANN (stacking of 20 networks), and (f) validation phase for INN14

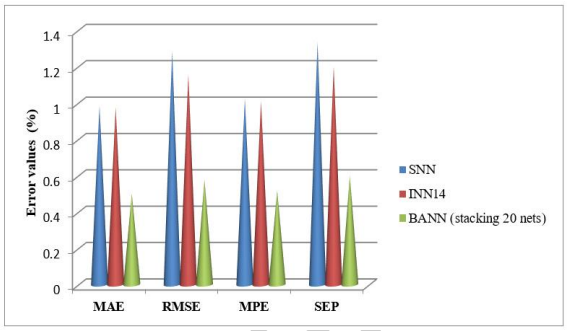

Figure 11. Comparison between errors values for the testing phase

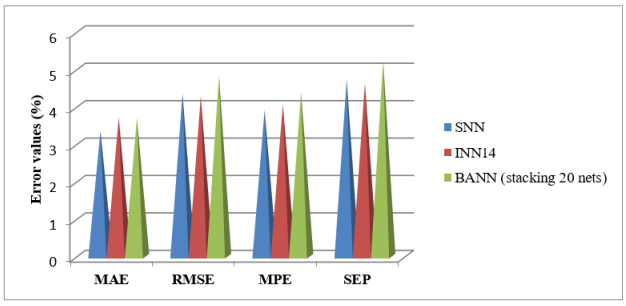

Figure 12. Comparison between errors values for the validation phase

The comparison between the three (03) models for the validation phase has been demonstrated in the next Figure 12. It can be seen that for the validation phase, the errors have near values, and the SNN gives the best precision with less value than the other models (BANN (stacking of 20 networks), and INN_{14}). The RMSE and SPE demonstrate that the INN_{14} has the best precision in comparison with the other models with values of more than 4% for all the models. MPE values are very close between them for the SNN and INN_{14}, for the BANN (stacking of 20 networks) the MPE value is more than 4%.

From the previous discussion, this comparison indicates the robustness, reliability, and efficiency nature of neural network models (QSPR-BANN (Stacking of 20 networks), QSPR-SNN, and QSPR-INN); it has demonstrated the superiority of the QSPR-BANN (Stacking of 20 networks) model. For the performance of the models, the QSPR-BANN (Stacking of 20 networks) model has the excellent precision and can predict the organic molecules rejection by the forward osmosis membranes, nevertheless, this model has less precision than the other models (QSPR-SNN and QSPR-INN_{14}) with the aim of the generalization ability of the NN models.

3.4. Comparison with other works

Many studies have been used the artificial neural network to develop the separation membranes process, for the best of our knowledge, our work is the first one consists to apply the bootstrap aggregated neural networks (BANN) to predict the rejection of the OM by the FO membranes, for this purpose, a comparison with other works applied these models (SNN and BANN) in other separation membranes process such as nanofiltration and reverse osmosis membrane is supported. Table 4 shows the aim of each study. This Table demonstrates that the Bootstrap aggregated neural network (BANN) gives results with higher performance and precision than the single neural networks in the first hand and proves the robustness and the accuracy of our model than the other works in the second hand.

Table 4. Overview of various works on models (BANN)

	Method	Membrane type	Database	Number of MO	R	RMSE (%)	MAE (%)
Khaoune *et al.* 2017	BANN	NF/RO	436	42	0.8156	7.7058	4.7350
Ammi *et al.* 2018	BANN	NF/RO	278	23	0.9836	2.5882	0.9878
Ammi *et al.* 2021	BANN	NF/RO	599	23	0.9603	1.0105	0.7916
Our work 2023	BANN	FO	193	53	0.9909	0.5764	0.5001

4. Conclusion

This work explores the application of the BANN in forward osmosis membranes process separation to predict the organic molecules rejection. However, many models have been developed, single Neural Network has been created with eleventh input including the properties of organic molecules, membrane characteristics, and operating conditions. The study of the effect of training algorithms, transfer functions, hidden neurons, and subdivisions of the database present the main of the first section.

The bootstrap aggregated neural networks were found by many resampling of the original database. Moreover, a comparison between the BANN (stacked of n networks) obtained describes that the BANN (stacked of 20 networks) is the most performance one than the others, the twenty (20) individual neural networks developed have different architectures which demonstrated the non-consistent of these models, among all of these models, the INN_{14} is the most performance one. The INN_{14}, the BANN (stacked of 20 networks), and the SNN were compared between them using the Coefficient Correlation "R", the Root Mean Squared Error "RMSE" with (R= 0.9401, and RMSE= 1.2826%) for the SNN, INN_{14} gives R equal to 0.9915 and "RMSE" with 1.1526%, and the BANN (stacked of 20 networks) offers R =0.9904, and RMSE= 0.5764% for the testing phase. This work also shows the precision, the robustness, reliability, and efficiency nature of each model generated using the Mean Absolute Error (MAE), the Root Mean Squared Error (RMSE), the Model Predictive Error (MPE), and the Standard Error of Prediction (SEP) with the outstanding superiority of the QSPR-BANN $_{(Stacking\ of\ 20\ networks)}$ model for the unseen data. This work demonstrates the excellence of our BANN model in comparison with other works that applied the Bootstrap aggregated neural networks method for the predicting of the organic molecules rejection by other separation membranes process such as nanofiltration and reverse osmosis. The bootstrap aggregated neural network gives honorable results for the prediction of the rejection of the organic molecules by the forward osmosis membranes in accordance with the other results of the same objective by other membranes (NF/RO) and with the advantage of the BANN compared to the Single Neural Networks for the unseen data.

Acknowledgments

The authors gratefully acknowledge the Ministry of Higher Education of Algeria (PRFU Projects N° A16N01UN260120220004) and the group of Laboratory of Biomaterials and Transport Phenomena in university of Medea.

Compliance with ethical standards

Conflict of interest Authors declares that there is no conflict of interest to declare.

References

Alturki A.A., McDonald J.A., Khan S. J., Price W.E., Nghiem L.D. and Elimelech M. (2013). Removal of trace organic contaminants by the forward osmosis process. *Separation and Purification Technology*. **103**. 258–266. DOI: 10.1016/j.seppur.2012.10.036.

Amiri B., Dizène R. and Dahmani K. (2020). Most relevant input parameters selection for 10-min global solar irradiation estimation on arbitrary inclined plane using neural networks. *International Journal of Sustainable Energy*. **39**(8), 779–803.

Ammi Y., Hanini S. and Khaouane L. (2021). An artificial intelligence approach for modeling the rejection of anti-inflammatory drugs by nanofiltration and reverse osmosis membranes using kernel support vector machine and neural networks. *Comptes Rendus. Chimie*. **24**(2). 243–254. DOI: 10.5802/crchim.76.

Ammi Y., Khaouane L. and Hanini S. (2015). Prediction of the rejection of organic compounds (neutral and ionic) by nanofiltration and reverse osmosis membranes using neural networks. *Korean Journal of Chemical Engineering*. **32**(11), 2300–2310. DOI: 10.1007/s11814-015-0086-y

Ammi Y., Khaouane L. and Hanini S. (2018). A model based on bootstrapped neural networks for modeling the removal of organic compounds by nanofiltration and reverse osmosis membranes. *Arabian Journal for Science and Engineering*. **43**(11). 6271–6284.

Ammi Y., Khaouane L. and Hanini S. (2020). A comparison of neural networks and multiple linear regressions models to describe the rejection of micropollutants by membranes. *Kemija u industriji: Časopis kemičara i kemijskih inženjera Hrvatske*. **69**(3–4). 111–127.

Ammi Y., Khaouane L. and Hanini S. (2021). Stacked neural networks for predicting the membranes performance by treating the pharmaceutical active compounds. *Neural Computing and Applications*. **33**(19): 12429–12444. DOI: 10.1007/s00521-021-05876-0.

Arcanjo G.S., Costa F.C., Ricci B.C., Mounteer A.H., D.E Melo E.N., Cavalcante B.F. and Amaral M.C. (2020). Draw solution solute selection for a hybrid forward osmosis-membrane distillation module: effects on trace organic compound rejection, water flux and polarization. *Chemical Engineering Journal*. **400**. 125857. DOI: 10.1016/j.cej.2020.125857

Barello M., Manca D., Patel R. and Mujtaba I.M. (2014). Neural network based correlation for estimating water permeability constant in RO desalination process under fouling. *Desalination*. **345**. 101–111. DOI: 10.1016/j.desal.2014.04.016.

Bowen W.R., Jones M. G., Welfoot J.S. and Yousef H.N. (2000). Predicting salt rejections at nanofiltration membranes using artificial neural networks. *Desalination*. **129**(2). 147–162.

Cath T.Y., Childress A.E. and Elimelech M. (2006). Forward osmosis: Principles, applications, and recent developments. *Journal of membrane science*. **281**(1–2). 70–87. DOI: 10.1016/j.memsci.2006.05.048.

Chung T.S., Zhang S., Wang K.Y., Su J. and Ling M.M. (2012). Forward osmosis processes: yesterday, today and tomorrow. *Desalination*. **287**. 78–81.

Cordier C., Guyomard K., Stavrakakis C., Sauvade P., Coelho F. and Moulin P. (2020). Culture of microalgae with ultrafiltered seawater: a feasibility study. *SciMedicine Journal*. **2**(2), 56–62.

Cui Y., Liu X., Chung Y.T.S., Weber M., Staudt C. and Maletzko C. (2016). Removal of organic micro-pollutants (phenol, aniline and nitrobenzene) via forward osmosis (FO) process: evaluation of FO as an alternative method to reverse osmosis (RO). *Water research*. **91**. 104–114. DOI. 10.1016/j.watres.2016.01.001

Darwish N.A., Hilal N., Al-Zoubi H. and Mohammad A. W. (2007). .Neural networks simulation of the filtration of sodium chloride and magnesium chloride solutions using nanofiltration membranes. *Chemical Engineering Research and Design*. **85**(4): p. 417–430.

Despotovic M., Nedic V., Despotovic D. and Cvetanovic S. (2015). Review and statistical analysis of different global solar radiation sunshine models. Renewable and Sustainable Energy Reviews, 52, 1869–1880. https://doi.org/10.1016/j.rser.2015.08.035

Dolar D., Zokić T. I., Košutić K., Ašperger D. and Pavlović D.M. (2012). RO/NF membrane treatment of veterinary pharmaceutical wastewater: comparison of results obtained on a laboratory and a pilot scale. *Environmental Science and Pollution Research*. 19(4). 1033–1042.

Dornier M., Decloux M., Trystram G. and Lebert A. (1995). Dynamic modeling of crossflow microfiltration using neural networks. *Journal of membrane science*. 98(3). 263–273.

Fissa M.R., Lahiouel Y., Khaouane L. and Hanini S. (2019). QSPR estimation models of normal boiling point and relative liquid density of pure hydrocarbons using MLR and MLP-ANN methods. *Journal of Molecular Graphics and Modelling*. 87. 109–120. DOI: 10.1016/j.jmgm.2018.11.013.

García-Alba J., Bárcena J.F., Ugarteburu C. and García A. (2019). Artificial neural networks as emulators of process-based models to analyse bathing water quality in estuaries. *Water research*. **150**, 283–295. DOI.10.1016/j.watres.2018.11.063

Gur-Reznik S., Koren-Menashe I., Heller-Grossman L., Rufel O. and Dosoretz C.G. (2011). Influence of seasonal and operating conditions on the rejection of pharmaceutical active compounds by RO and NF membranes. *Desalination,* **277**(1–3), 250–256.

Heo J., Kim S., Her N., Park C.M., Yu M. and Yoon Y. (2020). Removal of contaminants of emerging concern by FO, RO, and UF membranes in water and wastewater. *Contaminants of Emerging Concern in Water and Wastewater*. 139–176 DOI:10.1016/B978-0-12-813561-7.00005-5

Ibrar I., Yadav S., Altaee A., Braytee A., Samal A. K., Javaid S.M., and Hawari A.H. (2023). A machine learning approach for prediction of reverse solute flux in forward osmosis. Journal of Water Process Engineering, **54**, 103956.

Im S.J., Lee H. and Jang A. (2021). Effects of co-existence of organic matter and microplastics on the rejection of PFCs by forward osmosis membrane. *Environmental Research*. **194**, 110597.

Jamil S., Loganathan P., Kazner C. and Vigneswaran S. (2015). Forward osmosis treatment for volume minimisation of reverse osmosis concentrate from a water reclamation plant and removal of organic micropollutants. *Desalination*. **372**. 32–38.

Jawad J., Hawari, A.H. and Zaidi S. (2020). Modeling of forward osmosis process using artificial neural networks (ANN) to predict the permeate flux. *Desalination*. **484**: 114427. DOI: 10.1016/j.desal.2020.114427

Khaouane L., Ammi Y. and Hanini S. (2017). Modeling the retention of organic compounds by nanofiltration and reverse osmosis membranes using bootstrap aggregated neural networks. *Arabian Journal for Science and Engineering* **42**(4), 1443–1453.

Kim Y., Li S., Chekli L., Woo Y.C., Wei C.H., Phuntsho S. and Shon H. K. (2017). Assessing the removal of organic micro-pollutants from anaerobic membrane bioreactor effluent by fertilizer-drawn forward osmosis. *Journal of Membrane Science*. **533**. 84–95.

Kong F.X., Yang H.W., Wang X.M. and Xie Y.F. (2014). Rejection of nine haloacetic acids and coupled reverse draw solute permeation in forward osmosis. *Desalination*. **341**. 1–9.

Lanteri Y., Szymczyk A. and Fievet P. (2008) Influence of steric, electric, and dielectric effects on membrane potential. *Langmuir*. **24**(15), 7955–7962. DOI: 10.1021/la800677q.

Lee H., Im S.J., Park J.H. and Jang A. (2019). Removal and transport behavior of trace organic compounds and degradation byproducts in forward osmosis process: Effects of operation conditions and membrane properties. *Chemical Engineering Journal*. **375**. 122030.

Li C., Li H., Yang Y. and Hou L.A. (2020). Removal of pharmaceuticals by fouled forward osmosis membranes: Impact of DOM fractions, Ca2+ and real water. *Science of The Total Environment*. **738**. 139757. DOI: 10.1016/j.scitotenv.2020.139757

Linares R.V., Yangali-Quintanilla V., Li Z. and Amy G. (2011). Rejection of micropollutants by clean and fouled forward osmosis membrane. *Water research*. **45**(20). 6737–6744.

Lutchmiah K., Verliefde A.R.D., Roest K., Rietveld L.C. and Cornelissen E.R. (2014). Forward osmosis for application in wastewater treatment: A review. *Waterresearch*. **58**: 179197. DOI. 10.1016/j.watres.2014.03.045

Madaeni S., Shiri M. and Kurdian A. (2015). Modeling, optimization, and control of reverse osmosis water treatment in kazeroon power plant using neural network. *Chemical Engineering Communications*. **202**(1). 6–14. DOI: 10.1080/00986445.2013.828606

Madsen H.T., Bajraktari N., Hélix-Nielsen C., Van der Bruggen B. and Søgaard E.G. (2015). Use of biomimetic forward osmosis membrane for trace organics removal. *Journal of Membrane Science*. **476**. 469–474. DOI: 10.1016/j.memsci.2014.11.055

Maouz H., Hanini S.K.L. and Ammi Y. (2019). Modeling the molecular weight and number average molecular masses during the photo-thermal oxidation of polypropylene using neural networks. *Moroccan Journal of Chemistry*. **7**(1). 7–1. 017–027.

Martinetti C.R., Childress A.E. and Cath T.Y. (2009). High recovery of concentrated RO brines using forward osmosis and

membrane distillation. *Journal of membrane science*. **331**(1-2). 31–39.

McGinnis R.L. and Elimelech M. (2007). Energy requirements of ammonia–carbon dioxide forward osmosis desalination. *Desalination*. 207(1–3). 370–382. DOI:10.1016/j.desal. 2006.08.012

Mi B. and Elimelech M. (2010. Organic fouling of forward osmosis membranes: Fouling reversibility and cleaning without chemical reagents. *Journal of membrane science*. **348**(1–2), 337–345. DOI: 10.1016/j.memsci.2009.11.021.

Mohammad A.T., Al-Obaid M.A.I, Hameed E.M., Basheer B.N. and Mujtaba I.M. (2020). Modelling the chlorophenol removal from wastewater via reverse osmosis process using a multilayer artificial neural network with genetic algorithm. *Journal of Water Process Engineering*. **33**, 100993. DOI.org/10.1016/j.jwpe.2019.100993.

Nam S. N., Yea Y., Park S., Park C., Heo J., Jang, M. and Yoon Y. (2023). Modeling sulfamethoxazole removal by pump-less in-series forward osmosis–ultrafiltration hybrid processes using artificial neural network, adaptive neuro-fuzzy inference system, and support vector machine. Chemical Engineering Journal, 145821.

Pardeshi P.M., Mungray A.A. and Mungray A.K. **(**2016). Determination of optimum conditions in forward osmosis using a combined Taguchi–neural approach. *Chemical Engineering Research and Design*. **109**. 215–225. DOI: 10.1016/j.cherd.2016.01.030

Rastgar M., Shakeri A., Karkooti A., Asad A., Razavi R. and Sadrzadeh M. (2020). Removal of trace organic contaminants by melamine-tuned highly cross-linked polyamide TFC membranes. *Chemosphere*. **238**. 124691. DOI: org/10.1016/j.chemosphere.2019.124691

Santos J.L., de Beukelaar P., Vankelecom I.F., Velizarov S. and Crespo J.G. (2006). Effect of solute geometry and orientation on the rejection of uncharged compounds by nanofiltration. *Separation and purification technology*. **50**(1). 122–131.

Shaffer D.L., Werber J.R., Jaramillo H., Lin S. and Elimelech M. (2015) Forward osmosis where are we now? *Desalination*. **356**, 271–284.

Sharma S.K. and Tiwari K.N. (2009). Bootstrap based artificial neural network (BANN) analysis for hierarchical prediction of monthly runoff in Upper Damodar Valley Catchment. *Journal of hydrology*. **374** (3–4), 209-222. DOI: 10.1016/j.jhydrol.2009.06.003.

Shetty G.R., Malki H. and Chellam S. (2003). Predicting contaminant removal during municipal drinking water nanofiltration using artificial neural networks. *Journal of Membrane Science*. **212**(1–2). 99–112. DOI: 10.1016/S0376-7388(02)00473-8

Si-Moussa C., Hanini S., Derriche R., Bouhedda M. and Bouzidi A. (2008). Prediciton of high-pressure vapor liquid equilibrium of six binary systems, carbon dioxide with six esters, using an artificial neural network model. *Brazilian Journal of Chemical Engineering*. **25**(1). 183–199. DOI: 10.1590/S0104-66322008000100019.

Xie M., Nghiem L. D., Price W.E. and Elimelech M. (2012). Comparison of the removal of hydrophobic trace organic contaminants by forward osmosis and reverse osmosis. *Water research*. **46**(8). 2683–2692. DOI: 10.1016/j.watres.2012.02.023

Xie M., Nghiem L.D., Price W.E. and Elimelech M. (2014). Impact of organic and colloidal fouling on trace organic contaminant rejection by forward osmosis: Role of initial permeate flux. *Desalination*. **336**, 146–152. DOI: 10.1016/j.desal.2013.12.037

Xie M., Price W.E., Nghiem L.D. and Elimelech M. (2013). Effects of feed and draw solution temperature and transmembrane temperature difference on the rejection of trace organic contaminants by forward osmosis. *Journal of Membrane Science*. **438**. 57–64.

Yadav A.K. and Chandel S.S. (2014). Solar radiation prediction using Artificial Neural Network techniques. A review. Renewable and sustainable energy reviews. **33**, 772–781.

Yangali-Quintanilla V., Verliefde A., Kim T.U., Sadmani A., Kennedy M. and Amy G. (2009). Artificial neural network models based on QSAR for predicting rejection of neutral organic compounds by polyamide nanofiltration and reverse osmosis membranes. *Journal of membrane science*. **342**(1–2). 251–262. DOI: 10.1016/j.memsci.2009.06.048

Zhang J. (2008). Batch-to-batch optimal control of a batch polymerisation process based on stacked neural network models. *hemical Engineering Science*. 63(5), 1273–1281.

Zhang J., Jin Q. and Xu Y. **(**2006). Inferential estimation of polymer melt index using sequentially trained bootstrap aggregated neural networks. *Chemical Engineering & Technology: Industrial Chemistry-Plant Equipment-Process Engineering-Biotechnology*. **29**(4), 442–448.

Zhang Y., Gao X., Smith K., Inial G., Liu S., Conil L.B. and Pan B. (2019). Integrating water quality and operation into prediction of water production in drinking water treatment plants by genetic algorithm enhanced artificial neural network. *Water research*. **164**. 114888.

Zhao S. and Zou L. (2011). Effects of working temperature on separation performance, membrane scaling and cleaning in forward osmosis desalination. *Desalination*. **278**(1–3). 157–64.

Zhao S., Zou L., Tang C.Y. and Mulcahy D. (2012). Recent developments in forward osmosis: Opportunities and challenges. *Journal of membrane science*. **396,** 1–21.

Zheng L., Price W.E., McDonald J., Khan S.J., Fujioka T. and Nghiem L.D. (2019). New insights into the relationship between draw solution chemistry and trace organic rejection by forward osmosis. *Journal of Membrane Science*. **587**. 117184.